A Novel Look at Models for Polymer Entanglement

N. Heymans

Physique des Matériaux de Synthèse 194/08, Université Libre de Bruxelles, B-1050 Bruxelles, Belgium

Received July 20, 1999; Revised Manuscript Received November 22, 1999

ABSTRACT: Several apparently contradictory models predicting critical conditions for chain entanglement in flexible polymers have appeared in recent years. Some models predict entanglement molecular weight to increase, and others to decrease, with chain stiffness. Literature data are used here to compare model predictions. An inverse correlation between characteristic ratio and segmental aspect ratio is found, allowing the contradiction to be resolved. In flexible chains, it is found that the aspect ratio of a Kuhn step length is approximately independent of molecular characteristics and that stiffness depends more strongly on segmental aspect ratio than on characteristic ratio.

Introduction

It has been recognized for decades that entanglements are central to determining ultimate properties of flexible polymers such as craze draw ratio, failure mechanism, and molecular weight sensitivity of fracture stress, but that they also control low-strain properties such as the plateau modulus, steady-state compliance and zero-shear viscosity of polymer melts and solutions. However, the mechanism of entanglement in flexible polymers is still a matter of debate.

Early models of entanglements assumed localized entanglement "points", or temporary cross-links visualized as hooks, knots, or local interactions such as hydrogen bonding; however, Wolkowicz and Forsman[1] noted some years ago that the concept of "molecular weight between entanglements" is an oversimplification, leading to difficulty in reaching agreement between values of M_e obtained from different experiments on the same system. They introduced the concept of "partially entangled", "unentangled", and "fully entangled" normal modes, implying that entanglement only becomes fully effective beyond a certain length scale. Several later models treat entanglements as delocalized, nonspecific interactions, independent of the details of the structure and chemistry of the monomer. The nonlocalized character of entanglement interactions expresses itself through the differences in values of entanglement molecular weight M_e obtained from plateau modulus, critical molecular weight M_c obtained from viscosity, or characteristic molecular weight M'_c obtained from steady-state compliance.

The early models did not attempt to predict entanglement molecular weight M_e from first principles, but generally treated it as an adjustable parameter obtained experimentally from viscoelastic properties of the melt. Later models recalled below have linked the entanglement molecular weight to conformational characteristics of the polymer chain, in particular the characteristic ratio. These models may be qualified as topological or geometrical models as a whole. Since they are based on random chain statistics, they are clearly expected to apply only to flexible polymers.

At the present time models for entanglement onset can be classified in two schools. Wu[2] predicted, on the basis of a binary contact model, that the critical degree of polymerization for entanglement, N_c, should be proportional to C_∞^2. Wool[3] expressed that entanglement requires a chain to cross an arbitrary plane a critical number of times; this requires a critical number of Kuhn steps per entangled length and leads to proportionality between N_c and C_∞. Both models predict that closely coiled chains should be *more* entangled than straighter chains. These models will be called WW models from here on. Several other models, to be discussed more fully below, predict a *decrease* of entanglement molecular weight with increasing characteristic ratio, in keeping with the concept that flexible chains, which are closely coiled, interact little with other chains. These models will be called I (interactive) models. A convincing comparison of models has been carried out by Richter et al.[4] by measuring the correlation length in a single system in which C_∞ was modified through temperature variation; this comparison lends support to I models. This class of models, in particular the packing model, is supported by recent data of Fetters et al.[5−7] on a large number of polymers and systems having very different chain stiffnesses. On the contrary, Aharoni[8,9] established empirically, from his extensive compilation of chain stiffness parameters and entanglement molecular weights on a large number of polymers, that for flexible chains N_c increases as C_∞^2, and Wool's[3] data on a limited number of polymers supports his prediction N_c:C_∞.

In this paper, models predicting critical conditions for chain entanglement are analyzed in the light of Aharoni's compilation and also of the recent work of Fetters et al. Aharoni's data set is used, although it contains a number of discrepancies, because it is frequently cited in support of WW models; in fact, it will be shown that it supports I models equally well. The sources of this apparent paradox will be clarified below.

Entanglement Models and Chain Statistics

The Graessley−Edwards Analysis. Classical rubber elasticity treats a segment as a thin rod having length but no thickness or cross-sectional area. The appropriate segment in this context is clearly the Kuhn step length or the persistence length. Graessley and Edwards[10] noted that melt elasticity must involve two independent length scales, chose the Kuhn step length and the total contour length per unit volume, and showed by dimensional analysis that the plateau modulus can be expressed as

$$G_N^0 l_K^3/[kT] = f(\nu L l_K^2) \qquad (1)$$

10.1021/ma9911849 CCC: $19.00
Published on Web 05/12/2000

where l_K is the Kuhn step length, ν is the number of chains per unit volume, L is chain length, and νL is chain contour length per unit volume. Restricting the function f to a power law with exponent a, eq 1 can be expressed as

$$G_N^0 l_K^3/[kT] = (\nu L l_K^2)^a \quad (2)$$

In this relation, νL appears as a global quantity expressing chain packing density. Note, however, that it can also be expressed in terms of a local quantity, the cross-sectional area S_0 of a rigid unit. Since $\nu L S_0 = \phi$ (the polymer volume fraction), eq 2 can alternatively be written:

$$G_N^0 l_K^3/[kT] \propto (\phi l_K^2/S_0)^a \quad (3)$$

This can in turn be expressed in terms of polymer density ρ, volume fraction ϕ, rigid segment molecular mass and length M_0 and l_0, characteristic ratio C_∞, and Avogadro's number N_A:

$$G_N^0 \propto kTC_\infty^{2a-3}(\rho N_A \phi/M_0)^a l_0^{3a-3} \quad (4)$$

Graessley and Edwards eliminated G_N^0 by means of the reptation model, which gives the plateau modulus in terms of the tube diameter, identified with the end-to-end length r_e of an entangled strand, as

$$G_N^0 = \frac{4}{5}\frac{\rho N_A kT}{r_e^2}\frac{\langle R^2\rangle}{M} = \frac{4}{5}\frac{\rho N_A kT}{M_e} \quad (5)$$

where

$$\langle R^2\rangle/M = C_\infty l_0^2/M_0 \quad (6)$$

Introducing eq 5 into eq 4 thus gives the entanglement molecular weight in terms of rigid unit characteristics (subscript 0), characteristic ratio C_∞ and exponent a:

$$M_e \propto M_0 C_\infty^{3-2a}(\rho N_A \phi/M_0)^{1-a} l_0^{3-3a} = C_\infty^{3-2a}(l_0^2\phi/S_0)^{1-a} M_0 \quad (7)$$

Dimensional analysis alone cannot, of course, give a value for a; several models for entanglement onset lead to different exponents a, which will be compared below with experimental data from the litterature. Note that eq 7 relates three dimensionless ratios (excluding ϕ) but only requires one exponent a; this prediction, based on the assumption that the plateau modulus is proportional to l_K^3, is stronger than dimensional analysis alone, which would lead to an expression for M_e/M_0 with two independent exponents. Incompatibility between experimental exponents does not necessarily imply failure of scaling, but may simply indicate that eq 1 is not a simple power law.

Packing Models. The models recalled in the following sections do not refer specifically to the plateau modulus and could be expected to apply to M_e, M_c, or M'_c. For definiteness, the notation M_c will be used from this point on.

A first class of models, generally referred to as packing models,[5−7,11−16] assume that a strand becomes entangled when its ratio of pervaded over occupied volume reaches a critical value. Motion is unhindered at the segmental level (as in Wolkowicz and Forsman's[1] "unentangled modes"), but as the length of a strand increases, the number of available conformations is increasingly restricted by neighboring chains. Since occupied volume is linear in molecular weight, and pervaded volume increases as some higher power ($M^{3/2}$ for a Gaussian chain), this defines a critical molecular weight for entanglement to occur. The volume available to a strand of molecular weight M_s is

$$\nu_{occ} = (M_s/M_0)(l_0 S_0/\phi) \quad (8)$$

whereas the pervaded volume is proportional to r_s^3 where r_s is the root-mean-square end-to-end length of the strand

$$\nu_p = A(C_\infty M_s/M_0)^{3/2} l_0^3 \quad (9)$$

with A a geometrical factor of order 1. The packing ratio N_p of pervaded over occupied volume increases with the molecular weight of the strand; it is also the average number of different chains sharing the volume pervaded by the reference chain. The entanglement molecular weight corresponds to a critical packing ratio N_{pc}:

$$N_{pc} = AC_\infty^{3/2}(M_c/M_0)^{1/2}(l_0^2\phi/S_0) \quad (10)$$

For purposes of comparison between models, a reduced critical molecular weight μ will be defined for each model. For the packing model, the ratio

$$\mu_p = (M_c/M_0)(l_0^2\phi/S_0)^2 C_\infty^3 = N_{pc}^2 \quad (11)$$

should be a universal constant, independent of characteristic ratio and monomer aspect ratio. Identifying eq 7 with eq 11 shows that the exponent a for the packing model is 3.

Equation 11 can be elegantly recast in terms of the packing length p used by Fetters et al.[5−7] This parameter is defined as the ratio of the volume of a chain over its mean square end-to-end length, which is also the ratio of the cross-sectional area over l_K

$$p = \frac{M}{\rho N_A}\frac{1}{\langle R^2\rangle} = \frac{S_0}{C_\infty l_0} \quad (12)$$

leading to

$$\mu_p = M_c/\rho N_A p^3 \quad (13)$$

The packing length, although not proportional to the chain diameter, expresses the chain thickness: the ratio $(l_K/p)^{0.5}$ is the aspect ratio of the Kuhn segment.

Various interpretations of the critical ratio N_{pc} have been given: Rault[11,14] suggested that the ratio of occupied over pervaded volume at the entanglement molecular weight, i.e., $1/N_{pc}$, is approximately equal to the free volume fraction f_g at the glass transition; this condition would define a critical mobility at onset of entanglement and would also explain the variability of N_{pc} between polymers. This possibility is tested in Figure 1, taking f_g from Table 11-II of Ferry[17] and $1/N_{pc} = 1/\mu_p^{0.5}$ computed using eq 13 for data taken from Fetters[5] (filled triangles) and eq 11 for data taken from Aharoni[8,9] (open squares). (Details of the manner in which data were analyzed are given in the Discussion.) No correlation can be seen between these two parameters, suggesting that entanglement onset is not deter-

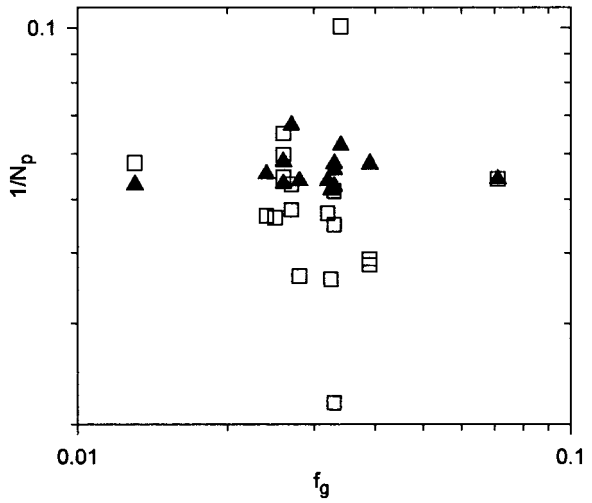

Figure 1. Reciprocal packing ratio vs free volume fraction f_g at T_g. f_g from Ferry,[17] packing ratio squares Aharoni,[8,9] triangles Fetters.[5]

mined by a critical mobility. Heymans[12] noted that the critical volume ratio also defines a critical ratio of end-to-end length over mean spacing, of order 3 for a series of amorphous polymers; her interpretation was that when a strand becomes entangled with surrounding chains, constraints from neighboring chains acting at either end of the strand become independent of each other. The average and standard deviation of this ratio, equal to $N_{pc}^{1/3}$, are in fact respectively 2.62 and 0.079 for the polymers investigated by Fetters,[5] and 2.99 and 0.53 for the flexible polymers in Aharoni's compilation. The ratio (2.99/2.62)[6] is approximately 2, which simply reflects the fact, discussed below, that most of Aharoni's data were obtained as $M_c = 2M_e$. (Note that a volume based model predicts neither a change nor anisotropy of entanglement density from affine deformation whereas a model based on the ratio of end-to-end length over mean spacing does, in conformity with experimental observations on changes in limiting extensibility after hot-drawing.[18,19]) Lin's[13] interpretation was in terms of a universal number of entanglement strands per cubed tube diameter; since the tube diameter is defined by entanglements formed by neighboring chains, this is simply an alternative formulation of the volume ratio concept. Fetters' interpretation is also simply in terms of the number of interacting chains in the volume pervaded by the reference chain.

Binary Contacts per Chain (EdG Model). Similar concepts underlie Edwards'[20] and de Gennes'[21] binary contact model, defining the onset of entanglement by a fixed number of binary contacts between Kuhn segments along an entangled length. This model is directly linked to the tube model: the entangled chain is "hedged in" by contacts with its neighbors. The number of Kuhn segments per unit volume is

$$c_K = \rho N_A \phi / M_0 C_\infty \tag{14}$$

The number of binary contacts per unit volume is given by this concentration, multiplied by the probability of finding another Kuhn segment in the immediate neighborhood of the segment. This probability is proportional to $c_K l_K^3$. The number of binary contacts per unit volume is then

$$n_b \propto c_K^2 l_K^3 \tag{15}$$

The number of entangled lengths per unit volume is

$$n_c = \rho N_A \phi / M_c \tag{16}$$

Combining the two preceding equations, the number of binary contacts $N_{bc} = n_b/n_c$ per entangled length, which is also the reduced entanglement molecular weight, is

$$\mu_{bc} = N_{bc} \propto \frac{\rho N_A \phi}{M_0} \frac{l_K^3}{C_\infty^2} \frac{M_c}{M_0} = \frac{\phi l_0^2}{S_0} C_\infty \frac{M_c}{M_0} \tag{17}$$

The exponent a in eq 7 for this model is 2. Equation 17 can also be recast in terms of the packing length, and of M_0 and l_0:

$$\mu_{bc} = M_c l_0 / [M_0 p] \tag{18}$$

The packing length, which appeared as a particularly appropriate parameter for describing the packing model, is insufficient in the context of the binary contact model; a second "local" parameter is required: the molecular weight per unit length of chain.

Binary Contacts per Pervaded Volume (CR Model). Colby et al.[22] combined the binary contact and packing concepts, suggesting that an entanglement is determined by a critical number of binary contacts in the volume pervaded by the entangled reference strand. This number is obtained by multiplying the number of binary contacts per unit volume, eq 15, by the pervaded volume, proportional to r_c^3, giving

$$n_v \propto c_K^2 l_K^3 r_c^3 = \left(\frac{\rho N_A \phi}{C_\infty M_0}\right)^2 C_\infty^3 l_0^3 \left(C_\infty \frac{M_c}{M_0} l_0^2\right)^{3/2} = \left(\frac{l_0^2 \phi}{S_0}\right)^2 \frac{M_c^{3/2}}{M_0} C_\infty^{5/2} \tag{19}$$

The reduced entanglement molecular weight is given by

$$\mu_C = (M_c/M_0)(l_0^2 \phi / S_0)^{4/3} C_\infty^{5/3} \tag{20}$$

and this model predicts an exponent a of $^7/_3$. In terms of the packing length, and molecular parameters, eq 20 becomes

$$\mu_C = M_c / [(\rho N_A)^{1/3} (M_0/l_0)^{2/3} p^{5/3}] \tag{21}$$

Wu's model. Using similar lines of thought as those underlying the EdG model, Wu expressed the number of Kuhn steps per unit length of chain as

$$n_K = 1/(l_0 C_\infty) \tag{22}$$

and stated that the number of binary contacts between Kuhn segments per unit length of chain is therefore proportional to n_K^2; if an entangled length contains N_c virtual bonds, there are $n_K^2 N_c l_0$ binary contacts per entangled length; a critical value for this number leads to the prediction that N_c should be proportional to C_∞^2, a result that appears to be in complete contradiction with eq 17. It may seem surprising that similar concepts should lead to such extremely different predictions of entanglement behavior; the caveat in Wu's derivation is that the number of binary contacts per unit length is porportional to, but not simply equal to n_K^2; this latter quantity cannot be a number per unit length since it

has dimensions L^{-2}. The correct derivation is the one given above, leading to eq 17. Wu's prediction is, however, supported by experimental data on 30 polymers. This point is discussed below.

Wool's Model. The basic concept in Wool's[3] model is that a chain is entangled if it crosses a load-bearing plane a sufficient number of times. If n_s is the number of chain segments crossing a plane, and n_c the number of chains crossing the same plane, entanglement requires $n_s > 3n_c$. From geometrical considerations, in the notations used here

$$n_c = 1.31[C_\infty/(M_0M)]^{1/2} l_0\rho \tag{23}$$

and $n_s = 1/S$, where S is the average segmental cross-section cut by the plane, defined from unit cell dimensions in order to account for local conformational characteristics of the chain

$$S = 2^{1/2} M_0 z/(\rho L) \tag{24}$$

where L/z is the c axis length per rigid unit. Solving for $M = M_c$ when $3n_cS = 1$ gives

$$M_c/M_0 = 30.89[l_0 z/L]^2 C_\infty \tag{25}$$

This concept in effect assumes similarity of all molecules at onset of entanglement, and effectively requires a universal number of Kuhn steps, leading to the prediction that N_c should be proportional to C_∞. It is interesting to note that, although the average cross-sectional area was formulated by Wool in terms of unit cell dimensions with the aim of accounting for the aspect ratio, this ratio has disappeared from the final result.

Discussion

Although all five models given above are based on scaling ideas, only the first three account for two independent length scales, expressed here via the aspect ratio of the rigid unit. These models, which could be qualified "full scaling" models, will be called I models for short hereafter. The data used here for evaluation of the models were obtained on bulk polymers, $\phi = 1$.

All three I models predict an increase in entanglement length with chain flexibility, in other words a flexible chain is less entangled than a less flexible one. Wu's prediction that the number of virtual segments between entanglements should *increase* like C_∞^2 was apparently supported by Aharoni's compilation of data on a number of flexible polymers, and Wool's prediction N_c proportional to C_∞ was supported by his own compilation. However, the basic concept underlying Wool's model, namely that a chain must cross a load-bearing plane three times to be able to transmit a load, is incompatible with the behaviour of immiscible systems compatibilized with block copolymers, where the greatest adhesive strength is obtained when each block is firmly embedded in the host polymer, i.e., when the copolymer chain crosses the load-bearing plane only once.

It may seem somewhat surprising that models leading to entirely contradictory predictions should apparently be convincingly supported by experimental evidence. In fact, this arises because a single parameter is insufficient to define molecular characteristics. As pointed out by Graessley and Edwards,[10] there are at least two independent length scales in the problem, which they took as the Kuhn step length and the total length of chain per unit volume; it was pointed out above that the latter ratio is equivalent to the reciprocal of the average cross-sectional area of the chain, so that the ratio l_k/NL used by Graessley and Edwards is equivalent to the ratio $l_k/S_0^{0.5}$ (or A/d) used by Aharoni.[8] However this latter ratio includes the characteristic ratio, so it is preferred in the present investigation to use the ratio $a_0 = l_0/S_0^{0.5}$, which is a direct property of the basic structural unit of the polymer.

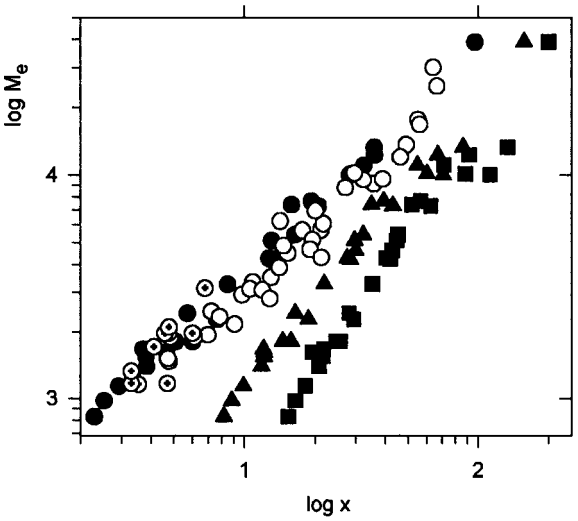

Figure 2. Entanglement molecular weight against denominator of eqs 13 (packing, circles), 18 (EdG, squares), and 21 (CR, triangles). Data from Fetters:[5] empty symbols, 298 K; filled symbols 413 K; cross-haired symbols, engineering polymers.

Fetter's Data. A compilation has been published recently by Fetters et al.,[5] incorporating data obtained in the same manner on the majority of polymers included in the compilation. Plateau moduli were obtained mainly from the area under the terminal loss peak, M_e was obtained from eq 5, and chain dimensions were obtained by SANS in the melt or from Θ-condition measurements. Details may be found in refs 5−7. The relevant data are given in Table 1; for the PEB series and the polydienes, M_0 and l_0 were calculated as average values per backbone bond. For the polydienes, it would be more appropriate to use the average rigid segment; this choice alters both M_0 and l_0. However, eqs 18 and 21 require only the ratio M_0/l_0, which is not much altered by the choice of base unit.

The scaling models predict that M_c (or M_e in the present case) should be linear respectively in $x = \rho N_A p^3$, $M_0 p/l_0$, and $(\rho N_A)^{1/3}(M_0/l_0)^{2/3}p^{5/3}$ following eqs 13, 18, and 21. Data are plotted in Figure 2 as M_e against the appropriate x, using logarithmic axes to avoid crowding; for the EdG and CR models only the 413 K data set are plotted to avoid clutter. This Figure shows that entanglement molecular weight is indeed proportional to x for the packing model, but varies as a higher power for the other scaling models. This appears more clearly in Figure 3, where the reduced entanglement molecular weight calculated from eqs 13 and 18 is plotted against packing length p; there is clearly no systematic dependence of μ_e on p for the packing model, whereas there is a distinct increase with p for the binary contact model. (A similar dependence is found for the CR model, but is not plotted for clarity.) Note that this is a particularly unflattering representation, which blows up data scatter, but also discriminates well between model predictions. Linear regression according to $M_e = ax + b$ gives

Table 1. Molecular Characteristics of Polymers from Fetters et al.[5]

polymer	$\langle R^2\rangle/M$	r	M_e	C_∞	M_0	l_0
			298 K			
alt-PEP	0.924	0.856	1475	6.99	17.95	1.54
PEB-17.6	0.926	0.860	1522	7.39	18.93	1.54
PEB-14	0.925	0.860	1522	6.99	17.92	1.54
PEB-24.6	0.800	0.864	2482	7.05	20.89	1.54
alt-PEB	0.725	0.861	2942	6.58	21.54	1.54
HHPP	0.691	0.878	3347	6.12	21	1.54
a-PP	0.664	0.852	3518	5.88	21	1.54
PEB-32	0.641	0.863	3888	6.21	22.96	1.54
PEB-39.3	0.623	0.864	4507	6.57	25	1.54
H2−50-PI	0.633	0.861	4876	9.34	35	1.54
PIB	0.570	0.918	5686	6.73	28	1.54
PEB-40.9	0.547	0.892	5709	5.87	25.450	1.54
H2−3,4-PI	0.464	0.878	9160	6.85	35	1.54
PEE	0.485	0.866	9536	5.52	27	1.54
PDMS	0.422	0.970	9613	5.77	37	1.645
1,4−1,2PBd	0.797	0.884	1947	5.60	27	1.960
62-PBd	0.727	0.890	2178	2.16	27	3.014
cis-PBd	0.758	0.900	2347	4.09	27	2.236
1,4-PEB	0.543	0.891	6090	4.19	41	2.305
cis-PI	0.679	0.913	3120	4.60	34	2.240
3,4-PI	0.563	0.890	5168	8.07	34	1.540
P2MP	0.585	0.850	4685	5.60	48	2.240
50-PI	0.546	0.893	4317	5.20	34	1.890
PVA	0.490	1.080	6944	8.88	43	1.540
55-DMBD	0.640	0.861	6257	7.50	26.45	1.503
PaMS	0.442	1.040	10225	11.0	59	1.54
PVE	0.664	0.889	3091	7.56	27	1.54
PMA	0.436	1.110	8801	7.91	43	1.54
H2−55-DMBD	0.431	0.838	13691	4.93	27.1	1.54
H2−1,4-MYRC	0.434	0.853	12077	6.41	35.03	1.54
PtBS	0.361	0.957	30108	12.2	80	1.54
1,4-MYRC	0.398	0.892	17681	6.11	34.01	1.49
H2−64-MYRC	0.409	0.849	16828	7.26	42.07	1.54
64-MYRC	0.374	0.891	24874	6.80	40.85	1.50
PPOX	0.599	1.00	2832	5.49	19.33	1.453
			413 K			
1,4-PI	0.625	0.830	5429	3.68	34	2.40
1,4-PBd	0.876	0.826	1815	4.04	27	2.42
PEB-2	1.210	0.785	976	7.43	14.56	1.54
PEB-4.6	1.150	0.788	1139	7.41	15.29	1.54
PS	0.434	0.969	13309	9.52	52	1.54
PVCH	0.323	0.920	38966	7.49	55	1.54
PEB-7.1	1.050	0.789	1398	7.08	15.99	1.54
PEB-11.7	0.952	0.793	1815	6.94	17.28	1.54
PEB-9.5	1.050	0.791	1552	7.38	16.66	1.54
PEB-10.6	1.060	0.792	1674	7.58	16.97	1.54
PMMA	0.425	1.130	10013	8.96	50	1.54
PEO	0.805	1.064	1624	5.59	14.67	1.453
PE	1.250	0.784	828	7.38	14	1.54
alt-PEP	0.834	0.790	2284	6.31	17.95	1.54
PEB-17.6	0.913	0.797	2433	7.29	18.93	1.54
PEB-24.6	0.799	0.799	3276	7.04	20.89	1.54
alt-PEB	0.692	0.800	4226	6.29	21.54	1.54
HHPP	0.691	0.810	4279	6.12	21	1.54
a-PP	0.670	0.791	4623	5.93	21	1.54
PEB-32	0.690	0.802	5124	6.68	22.96	1.54
PEB-39.3	0.645	0.805	7371	6.80	25	1.54
PIB	0.570	0.849	7288	6.73	28	1.54
PEB-40.9	0.604	0.805	7652	6.48	25.45	1.54
H2−3,4-PI	0.529	0.810	10114	7.81	35	1.54
PEE	0.507	0.807	11084	5.77	27	1.54
PDMS	0.457	0.895	12293	6.25	37	1.645
			Engineering Polymers			
RADEL-R	0.821	1.220	1240	2.00	133	7.39
Me-PEEK	0.834	1.160	1160	2.70	100.8	5.58
PET	0.844−0.949	0.989	1170	3.76−4.23	32	2.68
PC	0.864	1.14	1330	2.24	127	7.0
m-AEK	0.775	1.20	1720	2.70	85	4.94
PSF	0.699−0.756	1.15	1900	2.32−2.51	110	5.76
UDEL	0.699−0.756	1.16	1980	2.32−2.51	110	5.76
N6	0.853	0.985	1980	6.19	16.1	1.49
POM	0.763	1.142	2110	5.60	15	1.43
PPO	0.741	1.00	3150	3.05	120	5.40

[a] M_e, M_0 in g/mol; all lengths in Å

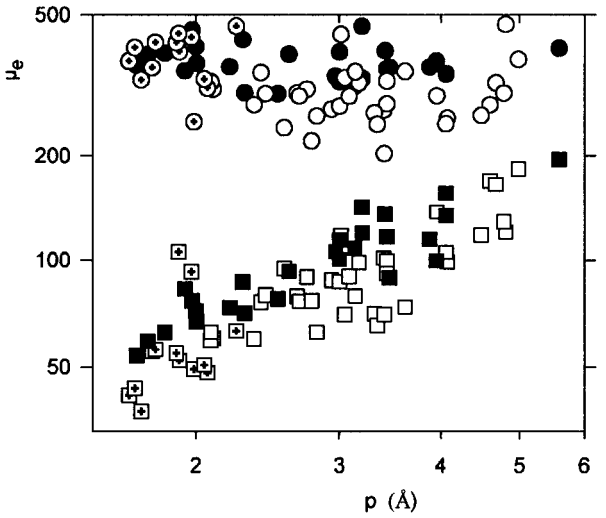

Figure 3. Reduced entanglement molecular weight against packing length. Data from Fetters;[5] symbols as Figure 2.

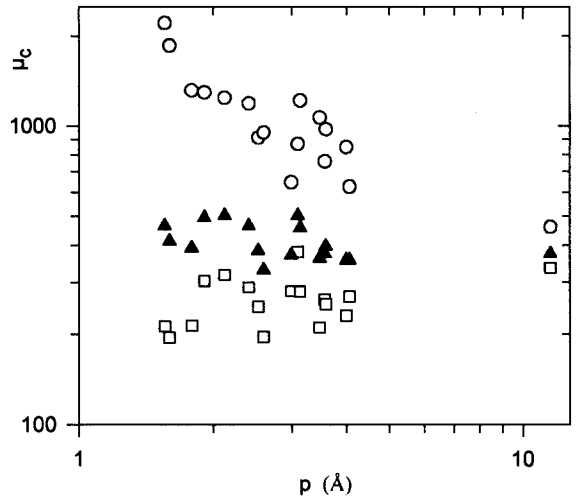

Figure 4. Reduced critical molecular weight. Data from Fetters:[7] circles, packing, eq 13; squares, EdG, eq 18; triangles, CR, eq 21.

Table 2. Linear Regression of M_e Following Eqs 13, 18 and 21 (r^2: Correlation Coefficient)

model	*a*	*b*	r^2
packing	361	−491	0.94
EdG	146	−2323	0.86
CR	207	−1918	0.93

the parameters and correlation coefficients in Table 2. This analysis is less discriminating than Figure 3, since it yields comparable correlation coefficients for the packing and CR models.

A similar plot is given in Figure 4 for Fetters et al.'s data[7] on critical molecular weight from viscosity. Although the number of reliable polymers is smaller for viscosity data, there is a clear downward and upward trend respectively for the packing and EdG models, and no particular trend for the CR model, which appears to be more appropriate than the packing model to describe viscosity data; thus the most adequate model depends on the property characterizing entanglement. Although this observation may seem surprising, it is in keeping with the dynamic nature of viscosity, which may be expected to depend more on the number of contacts between chains, and less on the number of available conformations, than melt elasticity. If this interpretation is correct, it is to be expected that the characteristic molecular weight from steady-state compliance should be best described by the EdG model. This might also explain why the results obtained by Richter et al.[4] seem to favor the CR model: these results were obtained by neutron spin echo measurements, and give a correlation length for dynamic events, rather than a "static" length scale such as the melt elasticity entanglement length.

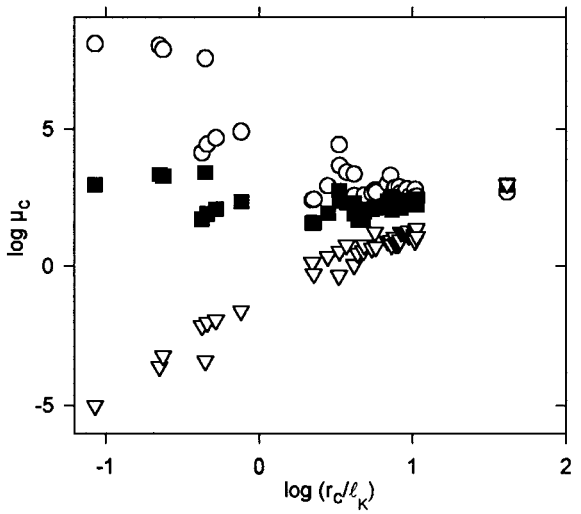

Figure 5. Dimensionless critical molecular weight against chain stiffness r_c/l_K. Data from Aharoni:[8,9] circles, packing, eq 11; squares, EdG, eq 17; empty triangles, Wu, N_c/C_∞^2.

Aharoni's Data. Fetter's data are clearly in favor of the packing model or the CR model; Aharoni's[8,9] data, frequently cited in support of WW models, will now be analyzed. Table 3 gives the relevant data; some polymers for which either C_∞ or S_0 were not given are excluded from the present analysis. The notations used here differ from those used by Aharoni: the subscript 0 refers here to the rigid unit, or virtual bond, whereas Aharoni used it to refer to a main chain bond. Our choice is in agreement with the definition of C_∞, and leads to values of N_c that are lower than those given by Aharoni for polymers with rigid moieties in the backbone. Also, d^2 in Aharoni's notation is S_0 here.

The models evaluated here are based on random chain statistics, and are only expected to apply to sufficiently long chains. The data are plotted in Figure 5 as reduced critical molecular weight against r_c/l_K, which is a measure of chain stiffness: $(r_c/l_K)^2$ is equal to the number of Kuhn segments per entangled length. The different symbols refer to eqs 11 (circles) and 17 (squares) and to Wu's prediction that $\mu_c = N_c/C_\infty^2$ (triangles). Wool's prediction and the CR prediction are not plotted to avoid clutter. If a model is correct, the corresponding μ_c should be independent of chain stiffness. There is a systematic rise of the "constant" for all three I models at high stiffness parameters (specifically, when the Kuhn step length becomes larger than the end-to-end distance of an entangled length); any model of entanglements based on chain statistics can be expected to break down when an entangled length contains fewer than one statistical segment! Wu's "constant" correlates very strongly with chain stiffness, particularly in the high stiffness range.

Since all models compared here were devised for flexible polymers, in all fairness rigid polymers should be excluded from the present analysis. Figure 6, identical to Figure 5 but including the CR prediction eq 20

Table 3. Molecular Characteristics of Polymers[a] from Aharoni[8,9]

no.	polymer	C_∞	M_0	M_c	l_0	r_c/l_K	S_0
	Rigid Polymers						
62	xanthan polysaccharide	750	555.91	3025	9.40	0.09	400.00
55	poly(*p*-phenyleneterephthalamide)	200	120.37	1200	6.50	0.22	38.47
57	poly(benzobisoxazole)	93	254.65	1320	12.20	0.24	36.60
53	(hydroxypropyl) cellulose (l.c. melt)	24.50	221.59	975	7.75	0.42	128.61
60	poly(*n*-butyl isocyanate)	500	75.00	7425	2.00	0.44	76.59
51	nitrocellulose	22	296.74	1365	7.75	0.46	78.50
52	cellulose acetate	23.40	281.25	1800	7.75	0.52	78.50
54	cellulose tributyrate	23	373.13	5000	7.75	0.76	85.00
	Semiflexible Polymers						
42	poly(2-methyl-6-phenyl-1,4-phenylene oxide)	3.70	182.40	3350	5.41	2.23	56.50
21	poly(acrylonitrile)	9.70	26.60	1330	1.54	2.27	30.85
43	poly(2,6dimethyl-1,4-phenylene oxide)	3.55	120.22	3360	5.41	2.81	35.52
23	PTFE	24	50.09	13225	1.54	3.32	27.08
41	polyestercarbonate 1 BPA, 2 terephthalic acid	3.30	129.92	4800	7.68	3.35	30.90
40	PC	2.40	146.67	4875	8.65	3.72	30.89
22	polyacrylamide	14.80	35.56	9140	1.54	4.17	45.20
16	poly(*N*-vinylcarbazole)	15.90	97.30	27050	1.54	4.18	131.02
20	poly(acrylic acid)	6.70	36.08	4690	1.54	4.40	45.20
8	1,2-polybutadiene	6.60	27.04	4110	1.54	4.80	49.88
38	PET	4.21	32.85	3270	2.14	4.86	20.00
	Flexible Polymers						
19	PVC	6.70	31.25	6250	1.54	5.46	27.18
44	poly(ether of BPA+diphenyl sulfone)	2	108.67	7070	5.76	5.70	30.90
4	hydrogenated poly(isoprene)	6.80	17.49	3970	1.54	5.78	28.50
46	poly(hexamethylene adipamide)	6.10	16.20	4730	1.49	6.92	17.60
2	PE	7	14.05	5115	1.54	7.21	18.28
3	PP	6.20	21.01	6890	1.54	7.27	34.27
30	poly(2-ethylbutylMA)	9.30	85.09	42800	1.54	7.35	100.00
45	poly(ϵ-caprolactam)	5.30	16.19	5020	1.49	7.65	17.86
6	c,t polybutadiene	5.50	13.50	4455	1.47	7.75	19.30
17	PVAc	9.40	43.05	24540	1.54	7.79	59.30
11	poly(α-methyl styrene)	10.50	59.13	40800	1.54	8.11	100
10	PS	10	52.01	35000	1.54	8.20	69.80
24	PMA	8	43.04	24100	1.54	8.37	59.30
31	PEO	4.20	14.70	4410	1.49	8.45	21.50
32	poly(propylene oxide)	5.10	19.38	7750	1.49	8.86	24.47
7	cis-polybutadiene	5.15	13.50	5940	1.47	9.24	20.70
25	PMMA	7	50.05	31530	1.54	9.49	63.84
9	cis-polyisoprene	5	17	7650	1.47	9.49	28
26	Pn-BMA	8	71.10	60435	1.54	10.31	93.60
27	Pn-HMA	10	85.09	91900	1.54	10.39	114.20
29	Pn-DodecMA	13.40	127.20	186350	1.54	10.46	176.60
1	PDMS	6	37.12	24500	1.46	10.49	43.60
5	polyisobutene	5	28.11	16020	1.54	10.68	41.24
28	P*n*-OctMA	10	99.13	114000	1.54	10.72	135.10
49	polymeric sulfur	1.76	32	96000	2.06	41.29	24.33

[a] M_c, M_0 in g/mol. All lengths in Å. Polymers sorted with increasing r_c/l_K

(filled triangles) and excluding polymers for which $r_c/l_K < 2$, rather unexpectedly shows no particular trend, but a good deal of scatter, for all three I models, and again a slight increase with flexibility for Wu's prediction. Some scatter arises from inappropriate values of C_∞, which do not all correspond to bulk or Θ-condition measurements. Also, several methods were used by the authors quoted by Aharoni to determine M_c. A few determinations were "direct", e.g., obtained from measurements of molecular weight dependence of melt viscosity; others were obtained from plateau modulus measurements, giving M_e via the rubber−elasticity relationship eq 5 (commonly used without the prefactor, although this is hardly likely to affect data scatter). This amounts to the assumption that melt elasticity is purely entropic, neglecting any energy contributions e.g. from interchain interactions or energy differences between conformers. Such contributions necessarily increase the modulus; thus, entanglement molecular weights obtained from melt elasticity measurements are likely to be underestimated; this effect is expected to increase with entanglement molecular weight, consistent with Richter et al.'s[4] observation that plateau modulus decreases more weakly than required by the increase of the entanglement distance. Also, different methods used in different sources for determining plateau modulus lead to inconsistencies between data for different polymers. Last, interconversion between M_c and M_e was carried out using the rule of thumb $M_c = 2M_e$; this is an additional source of scatter, since the ratio between M_c and M_e varies considerably between polymers.[23] More serious is the recent observation that this ratio is not random, but correlates with packing length;[7] this might affect not only the scatter, but also the trends of data with any parameter expressing chain flexibility. However, in view of the fact that most of Aharoni's data were obtained from M_e, any observable correlations are interpreted here as related to M_e rather than M_c.

An additional source of scatter arises, of course, from oversimplifications in the models themselves, which take into consideration only conformational contributions to entanglement, neglecting specific interactions, such as hydrogen bonding, polar interactions or local ordering. Such interactions are expected to decrease the

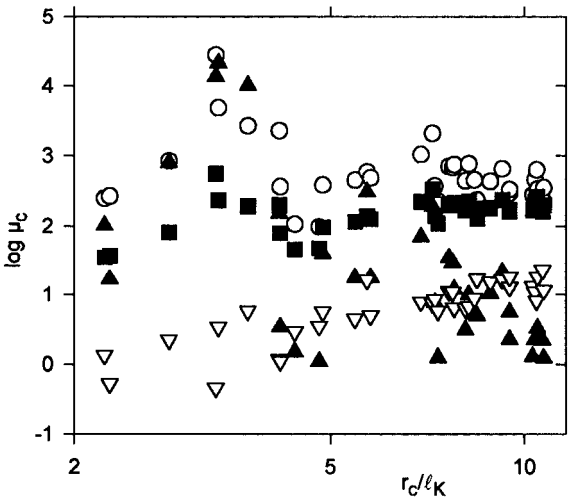

Figure 6. As in Figure 5, excluding rigid polymers (i.e., polymers having $r_c/l_K < 2$), and including CR, eq 20, empty triangles.

Table 4. Exponents of Eq 26 for Families of Polymers from Table 3 (r^2 = Correlation Coefficient)

	b	c	r^2	a_b	a_c
all	−3.87	−3.08	0.736	2.935	3.04
flexible	−3.25	−2.58	0.720	2.625	2.79
semirigid	−0.598	0.813	0.732	1.299	1.094
rigid	−3.37	−0.39	0.734	0.81	3.185
packing	−4	−3			3
binary contacts per chain	−2	−1			2
binary contacts per volume	−2.67	−1.67			$^7/_3$

molecular weight required for entanglement, but to be uncorrelated with geometrical characteristics of the base unit.

From visual inspection of Figure 6 scatter seems lowest for the EdG model, closely followed by packing. Evaluation of the models is refined here by expressing the critical number of rigid units in terms of the characteristic ratio and aspect ratio:

$$M_c/M_0 = A(l_0/S_0^{0.5})^b\, C_\infty^{\,c} \qquad (26)$$

The exponents are assumed here to be independent, to be able to check validity of eq 7. The data are separated, somewhat arbitrarily, into three groups on the basis of the value of the ratio $\lambda_c = r_c/l_K$: rigid ($\lambda_c < 1$), semirigid ($1 < \lambda_c < 5$) and flexible ($\lambda_c > 5$) polymers (the notation λ_c is used to recall that this ratio is, in fact, the maximum extensibility of an entangled length of chain). The values of the exponents b and c obtained by least-squares regression for the different groups of polymers are given in Table 4, together with the predictions of the scaling models and the scaling exponents a_b and a_c obtained from b and c by identifying exponents between eqs 7 and 26; compatibility with Graessley−Edwards scaling predictions is indicated by identity of a_b and a_c. These exponents are close to each other for the whole group of polymers, and for the flexible polymers alone, and are intermediate between the predictions of the packing models and the CR model. The semiflexible and rigid polymers both give incompatible values for the scaling exponent. This could simply mean that there are too few polymers in these groups for a valid statistical analysis. It could also mean that the exponents of C_∞ and of the segmental aspect ratio are not linked for these polymers, which in turn would be an indication that the plateau modulus is not determined by the Kuhn step length, as pointed out above. (This is indeed consistent with Aharoni's own observation that the plateau modulus correlates very poorly with M_c or N_c.) The correlation coefficients are low (approximately 0.85) for all groups of polymers, reflecting the considerable scatter.

Because of the deficiencies in Aharoni's data set, it does not allow clear discrimination between models; however, it lends at least as much support to I as to WW models.

The conclusion that a lies somewhere between the predictions of the packing and CR models is compatible with Colby et al.'s[22] analysis of a set of 13 polymers, where they found a minimum in the standard deviation for $a = 2.8$. Their method was different from ours, in that they assumed the exponents to be linked as in eq 7. They and Richter et al.[4] have also analyzed single−polymer data, in which M_c was varied by changing the temperature and hence C_∞ or by changing the concentration. Colby et al. obtained $a = 2.46$ from temperature dependence of M_e in poly(ethylenepropylene) (PEP), and Richter et al. found $a = 2.22$ from concentration dependence of the entanglement distance in the same polymer, but found that the invariants predicted by all scaling models were temperature-dependent. The value $a = 2.22$ was obtained assuming C_∞ was independent of concentration; if any swelling occurred this would lead to some compensation between decreasing concentration and increasing C_∞; accounting for this would increase the exponent.

Characteristic Ratio and Segmental Aspect Ratio. Although there remains some doubt as to which model is the best, and although the appropriate model appears to depend on the property under investigation, clearly any analysis of experimental data on flexible polymers leads to the conclusion that entanglement molecular weight decreases with increasing chain stiffness.

This is apparently in contradiction with WW models, and also with Wu's, Aharoni's and Wool's analysis of experimental data, which seem to confirm proportionality of M_c/M_0 to C_∞^2 or C_∞. The contradiction can be resolved, however, noting that the latter models only use one independent adimensional variable, whereas the scaling models require two, and hypothesizing that these two variables might not be mutually independent. This idea is tested in Figure 7, plotting C_∞ against segmental aspect ratio $a_0 = (l_0/S_0^{0.5})$, using data from Fetters and from Aharoni. C_∞ and S_0 are obtained from Fetters' data as $(\langle R^2\rangle/M)(M_0/l_0^2)$ and $M_0/(\rho N_A l_0)$. S_0 is not much influenced by the choice of base unit. This is not the case for C_∞, therefore these values were recalculated for the polydienes, taking a weighted average of C−C and C−C═C−C virtual bonds. The corresponding values of M_0 and l_0 are given in Table 5, and the data are not plotted in Figure 7, as these points fall well within the scatter range of the other data sets. For the flexible polymers, there is a clear inverse correlation between the two parameters, which is understandable since internal rotation is less hindered for long thin segments than for units with bulky side-groups. The correlation breaks down for very long thin rigid segments, since C_∞ cannot be lower than 2 (corresponding to a tetrahedral bond angle), and also for the polymers with very bulky side-groups, in which C_∞ is uncorrelated with segmental aspect ratio.

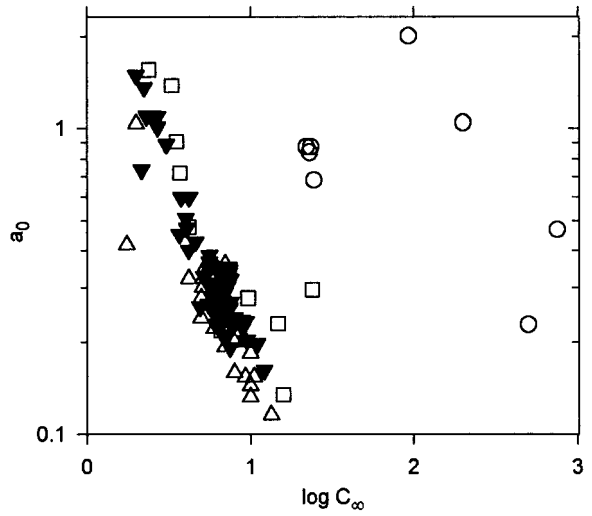

Figure 7. Correlation between segmental aspect ratio and C_∞. Aharoni: empty triangles, flexible; squares, semiflexible; circles, rigid. Fetters:[5] filled triangles.

Table 5. Average Virtual Bond Characteristics for Polydienes

polymer	M_0	l_0
1,4-PBd	14.21	1.49
1,4-PI	17.44	1.57
1,4−1,2PBd	16.88	1.50
62-PBd	19.57	3.06
cis-PBd	13.64	1.49
cis-PI	17	1.49
P2MP	24	1.49
50-PI	22.67	1.51
1,4-PEB	21.03	1.49

Least-squares regression gives C_∞:a_0^z with $z = -1.18$ for Fetters' data (filled triangles), −0.8 for the polydienes (diamonds), and −0.86 for Aharoni's flexible polymer data (empty triangles). The value found for this exponent has some interesting consequences. First, the exponent is close to −1; this means that the aspect ratio $a_K = (l_K/S_K^{0.5})$ of the Kuhn segment is nearly independent of the aspect ratio of the rigid unit and is determined mainly by geometrical considerations; specific interactions can only increase the stiffness. (If the cross-sectional area of the Kuhn segment is defined as volume over length, it is equal to that of the rigid segment, so $a_K = C_\infty a_0$.) Second, a somewhat counterintuitive result is that stiffness increases with decreasing C_∞: chain stiffness may be defined through the ratio $<R^2/M>$ which according to eq 6 is

$$\frac{\langle R^2\rangle}{M} = C_\infty\left(\frac{l_0}{S_0^{1/2}}\right)\frac{1}{\rho S_0^{1/2}} = \left(\frac{l_0}{S_0^{1/2}}\right)^a \frac{1}{\rho S_0^{1/2}} \qquad (27)$$

where a is close to nought. Chain stiffness thus increases for thin segments, which tend to be those with low characteristic ratios.

Third, if the exponent were exactly equal to −1, all three full scaling models would reduce to N_c:C_∞, i.e., Wool's prediction. With the extreme values of exponents 1.18 (0.8) obtained here, μ_c varies in a power of C_∞ equal to 0.39 (2), 0.69 (1.5), and 0.59 (1.67) for the packing, EdG and CR models respectively; consequently the same data set may appear to support WW and I models equally well, particularly if M_e or N_c is plotted linearly against the appropriate (or maybe inappropriate) variable. This does not imply that WW and I models are equally valid: the correlation between aspect ratio and characteristic ratio is far from perfect, therefore both ratios (or an equivalent pair of independent parameters) should appear explicitly in any sound prediction of entanglement molecular weight.

Conclusions

An analysis of Fetter's data, which clearly separates melt elasticity and viscosity measurements, demonstrates unequivocally that for sufficiently flexible polymers, the stiffer polymers are the more entangled. The packing model performs best for elasticity, and the Colby−Rubinstein model for viscosity.

A reappraisal of Aharoni's compilation of segmental and entanglement characteristics has been carried out. Because of data scatter and inconsistencies, different methods of analyzing data lead to different preferences of model, but these data also support the packing and CR models.

A correlation is found between the segmental aspect ratio and the characteristic ratio, leading to a Kuhn segment aspect ratio that depends very little on segmental geometry. One consequence of this correlation is that chain stiffness is inversely correlated with the characteristic ratio. This is perhaps the most important conclusion of this work, since it allows reconciliation of apparently contradictory predictions that have been a subject of heated debate over the past few years.

References and Notes

(1) Wolkowicz, R. I.; Forsman, W. C. *Macromolecules* **1971**, *4*, 184.
(2) Wu, Souheng *J. Polym. Sci., Part B: Polym. Phys.* **1989**, *27*, 723.
(3) Wool, R. P. *Macromolecules* **1993**, *26*, 1564.
(4) Richter, D.; Farago, B.; Butera, R.; Fetters, L. J.; Huang, J. S.; Ewen, B. *Macromolecules* **1993**, *26*, 795.
(5) Fetters, L. J.; Lohse, D. J.; Richter, D.; Witten, T. A.; Zirkel, A. *Macromolecules* **1994**, *27*, 4639.
(6) Fetters, L. J.; Lohse, D. J.; Graessley, W. W. *J. Polym. Sci., Polym. Phys. Ed.* **1999**, *3*, 1023.
(7) Fetters, L. J.; Lohse, D. J.; Milner, S. T.; Graessley, W. W. *Macromolecules* **1999**, *32*, 6847.
(8) Aharoni, S. M. *Macromolecules* **1983**, *16*, 1722.
(9) Aharoni, S. M. *Macromolecules* **1986**, *19*, 426.
(10) Graessley, W. W.; Edwards, S. F. *Polymer* **1981**, *22*, 1329.
(11) Rault, J. *C. R. Acad. Sc. Paris Ser. II* **1985**, *300*, 433.
(12) Heymans, N. *J. Mater. Sci.* **1986**, *21*, 1919.
(13) Lin, Y.-H. *Macromolecules* **1987**, *20*, 3080.
(14) Rault, J. *J. Non-Newton. Fluid Mech.* **1987**, *23*, 229.
(15) Kavassalis, T. A.; Noolandi, J. *Macromolecules* **1988**, *21*, 2869.
(16) Kavassalis, T. A.; Noolandi, J. *Macromolecules* **1989**, *22*, 2709.
(17) Ferry, J. D. *Viscoelastic Properties of Polymers*, 2nd ed.; John Wiley and Sons: New York, 1970.
(18) Heymans, N. *J. Mater. Sci.* **1988**, *23*, 2394.
(19) Heymans, N. *J. Polym. Sci., Part B: Polym. Phys.* **1990**, *28*, 951.
(20) Edwards, S. F. *Proc. Phys. Soc.* **1967**, *92*, 9.
(21) de Gennes, P.-G. *J. Phys. Lett.* **1974**, *35*, L-133.
(22) Colby, R. H.; Rubinstein, M.; Viovy, J.-L. *Macromolecules* **1992**, *25*, 996.
(23) Graessley, W. W. *The Entanglement Concept in Polymer Rheology*; Advances in Polymer Science; Springer: Berlin 1974; Vol. 16.

MA9911849